The Journal of Immunology

Anti-Inflammatory Role of the Murine Formyl-Peptide Receptor 2: Ligand-Specific Effects on Leukocyte Responses and Experimental Inflammation

Neil Dufton, Robert Hannon, Vincenzo Brancaleone, Jesmond Dalli, Hetal B. Patel, Mohini Gray, Fulvio D'Acquisto, Julia C. Buckingham, Mauro Perretti and Roderick J. Flower

J Immunol 2010; 184:2611-2619; Prepublished online 27 January 2010;
doi: 10.4049/jimmunol.0903526
http://www.jimmunol.org/content/184/5/2611

The Journal of Immunology is published twice each month by
The American Association of Immunologists, Inc.,
1451 Rockville Pike, Suite 650, Rockville, MD 20852

Print ISSN: 0022-1767 Online ISSN: 1550-6606.

Anti-Inflammatory Role of the Murine Formyl-Peptide Receptor 2: Ligand-Specific Effects on Leukocyte Responses and Experimental Inflammation

Neil Dufton,* Robert Hannon,* Vincenzo Brancaleone,* Jesmond Dalli,* Hetal B. Patel,* Mohini Gray,† Fulvio D'Acquisto,* Julia C. Buckingham,‡ Mauro Perretti,*,[1] and Roderick J. Flower*,[1]

The human formyl-peptide receptor (FPR)-2 is a G protein-coupled receptor that transduces signals from lipoxin A_4, annexin A1, and serum amyloid A (SAA) to regulate inflammation. In this study, we report the creation of a novel mouse colony in which the murine FprL1 FPR2 homologue, Fpr2, has been deleted and describe its use to explore the biology of this receptor. Deletion of murine *fpr2* was verified by Southern blot analysis and PCR, and the functional absence of the G protein-coupled receptor was confirmed by radioligand binding assays. In vitro, $Fpr2^{-/-}$ macrophages had a diminished response to formyl-Met-Leu-Phe itself and did not respond to SAA-induced chemotaxis. ERK phosphorylation triggered by SAA was unchanged, but that induced by the annexin A1-derived peptide Ac2–26 or other Fpr2 ligands, such as W-peptide and compound 43, was attenuated markedly. In vivo, the antimigratory properties of compound 43, lipoxin A_4, annexin A1, and dexamethasone were reduced notably in $Fpr2^{-/-}$ mice compared with those in wild-type littermates. In contrast, SAA stimulated neutrophil recruitment, but the promigratory effect was lost following Fpr2 deletion. Inflammation was more marked in $Fpr2^{-/-}$ mice, with a pronounced increase in cell adherence and emigration in the mesenteric microcirculation after an ischemia–reperfusion insult and an augmented acute response to carrageenan-induced paw edema, compared with that in wild-type controls. Finally, $Fpr2^{-/-}$ mice exhibited higher sensitivity to arthrogenic serum and were completely unable to resolve this chronic pathology. We conclude that Fpr2 is an anti-inflammatory receptor that serves varied regulatory functions during the host defense response. These data support the development of Fpr2 agonists as novel anti-inflammatory therapeutics. ***The Journal of Immunology*****, 2010, 184: 2611–2619.**

The polymorphonuclear leukocyte (PMN) is the first WBC type to egress from the blood during acute inflammation, followed by the monocyte (1). This process is orchestrated by the timed expression of cell-associated and soluble mediators, including adhesion molecules and cytokines or chemokines. At the site of inflammation, PMN life span is increased from hours to days, and monocytes differentiate into macrophages (Mϕs) to direct a series of events leading to safe resolution of the inflammatory process, with removal of the initial insult and restoration of tissue homeostasis (1, 2).

Because they transduce the action of chemokines and other inflammatory signals that are central to the adaptive and innate immune responses (3, 4), the role of G protein-coupled receptors (GPCRs) in host defense has been the object of intense scrutiny.

The concept that acute inflammation resolves through active processes is relatively novel (2, 5). An important function, in this context, is served by the arachidonate derivative lipoxin A_4 (LXA_4) (6) and by the glucocorticoid-modulated protein annexin A1 (AnxA1) (7), both of which operate in the inflamed tissue in a temporal and spatial fashion. LXA_4 and AnxA1 exert exquisite control over PMN biology, potently inhibiting cell interaction with the vascular endothelium and, at the site of inflammation, promoting apoptosis, phagocytosis, and egress (8–10). The major anti-inflammatory properties of LXA_4, aspirin-triggered LXA_4, and AnxA1 on PMNs are mediated through a specific GPCR, termed formyl peptide receptor (FPR) 2/LXA_4 receptor (ALX) (11).

Human FPR2/ALX, FPR, and FPR3 form a subgroup of receptors (12) linked to inhibitory G proteins so that their activation leads to transient calcium fluxes, ERK phosphorylation (13), and in some cases cell locomotion (14).

FPR2/ALX seems unusual, being used by both lipid and protein ligands (11, 12, 15). Not only does it transduce the anti-inflammatory effects of LXA_4 in many systems (8) as well as the neuroprotective effects of humanin (16) but it also can mediate proinflammatory responses to serum amyloid A (SAA) and other peptides (13, 17, 18). The ability of FPR2/ALX to mediate two opposite effects may be traced to different receptor domains used by different agonists (19).

*The William Harvey Research Institute, Barts and The London School of Medicine, Queen Mary University of London; ‡Office of Pro-Rector (Education), Imperial College London, London; and †Medical Research Council Centre for Inflammation, Edinburgh, United Kingdom

[1]M.P. and R.J.F. contributed equally to this work.

Received for publication October 28, 2009. Accepted for publication December 25, 2009.

This work was supported by The Wellcome Trust (Grants 086867/Z/08 and 069234/Z/02) and a studentship from the Research Advisory Board of Barts and the London and the Medical Research Council. This work forms part of the research themes contributing to the translational research portfolio of Barts and the London Cardiovascular Biomedical Research Unit, which is supported and funded by the National Institutes of Health Research.

Address correspondence and reprint requests to Prof. Roderick J. Flower, William Harvey Research Institute, Barts and The London School of Medicine, Queen Mary University of London, Charterhouse Square, London EC1M 6BQ, United Kingdom. E-mail address: r.j.flower@qmul.ac.uk

Abbreviations used in this paper: Ac2–26, peptide Ac2–26 of annexin A1; ALX, lipoxin A_4 receptor; AnxA1, annexin A1; Cpd43, compound 43; fMLP, formyl-Met-Leu-Phe; Fpr, formyl-peptide receptor; GPCR, G protein-coupled receptor; hrAnxA1, human recombinant annexin A1; LXA_4, lipoxin A_4; Mϕ, macrophage; PMN, polymorphonuclear leukocyte; SAA, serum amyloid protein A; WT, wild-type.

www.jimmunol.org/cgi/doi/10.4049/jimmunol.0903526

There are no specific antagonists or neutralizing Abs that can be used to delineate the function of FPR2/ALX in vivo (12), so most notions concerning its function have been inferred from in vitro studies that may not reflect the true role of this receptor in the complex and dynamic environment of an ongoing inflammatory response. To address this important question, we therefore have generated a novel mouse line in which the gene for Fpr2 [the murine homologue of FPR2/ALX, formerly referred to as Fpr-rs2 (20)] has been deleted. Fpr2 has 76 and 63% identity with human FPR2/ALX and FPR3, respectively (12, 21), and is known to be activated by SAA (22) and LXA_4 (23). Our aim was to determine the function of this receptor in inflammation as well as in response to natural and synthetic ligands.

Materials and Methods

Fpr2 ligands and reagents

GST-tagged human recombinant annexin A1 (hrAnxA1), produced in *Escherichia coli*, was purified protein by Sepharose column purification using GSTrap (GE Healthcare, Little Chalfont, U.K.). Endotoxin was monitored and found to be below detectable levels (0.05 endotoxin U/ml) using the E-Toxate kit (Sigma-Aldrich, St. Louis, MO). W-peptide and peptide Ac2–26 of annexin A1 (Ac2–26; acetyl-AMVSEFLKQAWIE-NEEQEYVVQTVK; M_r 3050) were synthesized by (Cambridge Bioscience, Cambridge, U.K.). LXA_4 was purchased from Calbiochem (San Diego, CA). IL-1β and SAA were purchased from PeproTech (Rocky Hills, NJ). Formyl-Met-Leu-Phe (fMLP), zymosan A, and dexamethasone 21-phosphate disodium salt were purchased from Sigma-Aldrich. Compound 43 (Cpd43) was a generous gift from Amgen (Thousand Oaks, CA).

Generation of the Fpr2$^{-/-}$ mouse

Fpr2$^{-/-}$ mice were generated by homologous recombination in embryonic stem cells using a dual purpose targeting/reporter vector. Genomic clones containing *Fpr* sequences were isolated from a bacteriophage λ library (129/SvJ; Stratagene, La Jolla, CA) by plaque hybridization. Inserts from positive plaques were subcloned into pZero (Invitrogen, Carlsbad, CA), end-sequenced, and then aligned with the fpr locus on chromosome 17. A pgk-neo cassette was inserted into one of these clones (p2.1) just downstream of the ATG start codon for *Fpr2*, using the technique of site-specific recombination in bacteria. The sequences of the primers used to achieve this step were forward 5′-tcagaaggagccaaatatctgagaaatggttgtttttgaaaactttcaggtgcagacaaaATGgctagcccttctgcttaatttgtgcctgg and reverse 5′-tgctgtgaaagaaaagtcagccaatgctagattcagataccagatagtggtgacagtgtgtggcgtagaggatctgcltcatgtttgac. With the plasmid pPGK-neo-FRT as a template for PCR, these primers amplified a fragment of 2.2kb containing the pgk-neo cassette in reverse orientation, flanked by 63-bp arms showing homology to Fpr2. This fragment was electroporated along with plasmid p2.1 into *E. coli* strain HS996 using the RED-ET subcloning kit supplied by Gene Bridges (Heidelberg, Germany). The novel NheI site (gctagc) located immediately after the ATG start codon in the forward primer was used for the subsequent in-frame insertion of GFP (Qbiogene, Irvine, CA) and also to facilitate Southern blot screening. All of the steps were confirmed by sequencing.

The targeting vector was linearized by digestion with SnaBI and electroporated into embryonic stem cells (strain 129SvEv). Neomycin-resistant colonies were picked and screened for correct insertion by Southern blot analysis using probes located beyond both the 5′ and 3′ ends of the vector arms and also a probe for GFP. Clones showing homologous recombination into the Fpr2 locus were expanded, karyotyped by G-banding, and then injected into the blastocysts of C57Bl6 females (Caliper Life Sciences, Cambridge, MA).

Male chimaeras showing >95% agouti coat color were paired with C57Bl6 females. F1 offspring were screened by PCR of tail clip DNA for germline transmission of the targeted allele using the Extract-N-Amp system (Sigma-Aldrich). The primers used for genotyping were F1 (tgagtgtcatgtcagaaggagcc), B11 (cggaatccagctacccaaatc), and GB4 (ataaccttcgggcatggcactc). The F1/B11 pair produces a band of 233 bp from the wild-type (WT) allele, whereas F1 and GB4 produce a band of 351 bp if the targeted allele is present. Cycling conditions were 92°C for 30s, 54°C for 15 s, and 72°C for 15 s for 33 cycles. Heterozygotes were mated to produce F2 homozygotes. Genotyping was performed by PCR and confirmed by Southern blot analysis (Fig. 1).

Genotype and litter size data on Fpr2$^{-/-}$ mice (16 litters, ~100 animals) confirmed that the gene assorted according to the expected Mendelian ratio and that there were no breeding abnormalities. The transgenic mice were viable, fertile, and showed no obvious developmental or behavioral defects. Similarly, no significant differences in the numbers of peritoneal resident cells (~4×10^6) or bone marrow or circulating PMNs were evident between WT littermate and Fpr2$^{-/-}$ mice (~20×10^6 and ~2.5×10^6 cells per milliliter, respectively; $n = 6$ mice per group).

Cellular and biochemical analyses

Preparation of Mϕs. Identical results were obtained using either bone marrow or peritoneal Mϕs. Bone marrow Mϕs were obtained from femurs and tibias of 4–6-wk-old WT littermate controls and Fpr2$^{-/-}$ mice. The marrow was flushed from the bone, washed, resuspended (2×10^6 cells per milliliter) in DMEM supplemented with L-glutamine, penicillin/streptomycin (Lonza Biologics, Slough, U.K.), 20% FCS, and 30% L929 conditioned medium, and incubated at 37°C for 5 d. Biogel-elicited Mϕs were harvested 4 d after i.p. injection of 1 ml, 2% P-100 gel (Bio-Rad, Hercules, CA) in sterile PBS. Cell suspensions were passed through 40-μm cell strainers (BD Biosciences, San Jose, CA) before being washed and seeded.

Mϕ chemotaxis. The commercially available Neuroprobe ChemoTx 96-well plate (Receptor Technologies, Leamington Spa, U.K.) with polycarbonate membrane filters and 5-μm membrane pores was used. Mϕs were resuspended at a concentration of 4×10^6 cells per milliliter in RPMI 1640 containing 0.1% BSA. The chemotaxis assay was performed by adding chemotactic stimuli to the bottom wells, with 10^5 Mϕ cell suspension in 25 μl placed above the membrane. Plates were incubated for 120 min in a humidified incubator at 37°C with 5% CO_2. Migrated cells were quantified after 4 h of incubation with alamarBlue (Serotec, Oxford, U.K.) by comparison with a standard curve constructed with known Mϕ numbers (range 0–4×10^6). Plates were read at 530–560 nm excitation and 590 nm emission wavelengths for fluorescence values.

Radioligand binding assays. These were conducted as described previously (24). Briefly, primary peritoneal Mϕs were resuspended at a concentration of 10×10^6 cells per milliliter in PBS containing Ca^{2+} and Mg^{2+} and placed on ice. The tracer ([^{125}I]W-peptide) was prepared following manufacturer's instructions (Phoenix Pharmaceuticals, Belmont, CA) and dissolved in 1 ml distilled water.

The unlabeled W-peptide also was dissolved in distilled water to a final concentration of 1 μM. Subsequently a 500 μM working stock was prepared; this was used to determine the extent of nonspecific binding by the radiolabeled tracer. Together with total binding of the tracer; specific binding can be estimated by total binding minus nonspecific binding.

The reaction mixture then was incubated for 1 h on ice, after which it was transferred to a vacuum filtration unit equipped with 25-mm GF/C filter membranes onto which any cells and bound tracer would be retained. The filters then were washed three times using 4 ml aliquots of 10 mM ice-cold Tris-HCl to remove any unbound tracer. After the wash step, the filter paper was transferred into recipient tubes, and the amount of bound tracer was determined using a γ-counter. This experiment was repeated three times to confirm the reproducibility of the results obtained.

Phospho-ERK signaling. Peritoneal Mϕs were equilibrated for 30 min in Glutamax DMEM (Invitrogen) supplemented with 50 U penicillin/streptomycin prior to incubation with the specified ligands in six-well plates for 10 min at 37°C. Mϕ lysates were analyzed by standard SDS-PAGE and transferred to polyvinylidene difluoride membranes (Millipore, Bedford, MA). Blots were probed for rabbit anti–phospho-p44/42 MAP L(polyclonal anti–phospho-ERK; 1:1000 dilution) or p44/42 MAPK Abs (total ERK, 1:1000 dilution; clone 137F5; Cell Signaling Technology, Beverly, MA) was diluted in 0.3% BSA/Tween 20 and Tris-buffered saline and incubated with the membrane overnight. Membranes were further incubated with HRP-conjugated goat anti-rabbit (DakoCytomation, Carpinteria, CA) and proteins were detected by ECL visualized on hyperfilm (GE Healthcare).

Histology. Analysis was conducted at the 4 h time point: joints were trimmed, placed in decalcifying solution (0.1 mM EDTA in PBS) for 25 d and then embedded in paraffin. Sections (5 μm) were deparaffinized with xylene and stained with H&E. Three sections per animal were evaluated. Phase-contrast digital images were taken using the Image Pro image analysis software package.

Inflammation assays

IL-1β–induced air pouch and zymosan-induced peritonitis. The air-pouch procedure was carried out as described previously (25), injecting 20 ng mouse IL-1β (PeproTech) in 0.5% carboxymethyl cellulose on day 6 after air-pouch induction. Zymosan peritonitis was induced by injecting i.p. 1 mg zymosan A (Sigma-Aldrich) in 0.5 ml PBS as previously described (26). Compounds were given i.v. immediately before IL-1β or zymosan. In all of the cases, either air pouches or peritoneal cavities were lavaged 4 h

later using 2 or 3 ml, respectively, PBS-containing 25 U/ml heparin and 0.3 mM EDTA. Exudate fluids were stained with Turk's solution to allow identification of differential PMN and PBMC counts in the total cell population by light microscopy. Proportions of specific leukocyte populations were confirmed and quantified by FACS (see below).

Carrageenan-induced paw edema. Paw edema was induced as previously described (27). Briefly, animals received subplantar administration of 50 μl carrageenan 1% (w/v) in saline. The volume was measured by using a hydroplethysmometer with mice paw adaptors (Ugo Basile, Varese, Italy) immediately before subplantar injection and 1, 2, 4, 6, and 8 h thereafter. Changes in paw volume were calculated by subtracting the initial paw volume (basal) from the paw volume measured at each time point.

Intravital microscopy of the mesenteric microcirculation. Intravital microscopy was performed as previously reported (28). Briefly, following anesthesia, cautery incisions were made along the abdominal region, and the superior mesenteric artery was clamped with a microaneurysm clip (Harvard Apparatus, Edenbridge, U.K.) to induce ischemia in the mesentery for 30 min prior to a 45 min reperfusion phase. Sham-operated mice were subject to anesthesia and other surgical procedures without clamping of superior mesenteric artery and analyzed 75 min after laparotomy. Mesenteries were superfused with thermostated (37°C) bicarbonate-buffered solution [7.71 g/l NaCl, 0.25 g/l KCl, 0.14 g/l $MgSO_4$, 1.51 g/l $NaHCO_3$, and 0.22 g/l $CaCl_2$ (pH 7.4), gassed with 5% CO_2/95%N_2] at a rate of 2 ml/min. One to three randomly selected postcapillary venules (diameter between 20 to 40 μm; visible length of at least 100 μm) were observed for each mouse (minimum of five animals per genotype). Leukocyte adhesion was measured by counting static (at least 30 s) cells clearly visible on the vessel wall in a 100 μm stretch. Leukocyte emigration from the microcirculation into the tissue was quantified by counting the number of cells in a 100 × 50 μm^2 area outside the vessel.

All of the animal studies were conducted in accordance with current U.K. Home Office regulations and complied with local ethical and operational guidelines.

K/B × N serum-induced inflammatory arthritis

Arthritis was induced by injection, on day 0, of 150 μl pooled K/B × N arthrogenic serum (29). Disease development was monitored by assessing the clinical index: one point was given for each digit, tarsal, or wrist joint that presented with erythema plus swelling; a maximum of 22 points could be scored per animal. Cumulative disease incidence was determined by the number of mice that presented a minimum of two paws with a clinical score and quantified as a percentage of the total group.

FACS analysis

Measurement of Fpr2 promoter activity and cell infiltrate by FACS. FACS analysis was used to assess the fluorescence of both stained and unstained cell populations. $Fpr2^{-/-}$ animals carried GFP within the promoter region of *Fpr2* and therefore allowed analysis of both constitutive and induced promoter activities in naive, differentiating, and inflammatory cell populations by FL-1 analysis. This methodology also was used to confirm genotypes.

Quantification of specific leukocyte populations. Specific leukocyte populations were identified using the following conjugated monoclonal Abs (all at 10 μg/ml final concentrations): anti-mouse Ly-6G/Gr1$^+$ (clone RB6-8C5; eBioscience, San Diego, CA), anti-mouse F4/80 (clone MCA497; Serotec), or isotype controls (eBR2a; eBioscience,) for 1 h at 4°C. Cell populations were analyzed for 10,000 events by FACSCalibur flow cytometry using CellQuest software (BD Biosciences). The percentage of total events in each population was compared with total cell count to calculate specific cell infiltrate per cavity or pouch.

Statistical analysis

Data are expressed as mean ± SEM. Student *t* test was used to compare two groups with parametric data distributions. Mann-Whitney *U* test was used for nonparametric data, such as the analysis for the ERK phosphorylation assays. Comparison between groups (e.g., of clinical scores and paw volumes) was made using ANOVA. All of the analyses were performed using GraphPad Prism 4.0 software (GraphPad, San Diego, CA). In all of the cases, a p value < 0.05 was taken as significant.

Results

Generation and validation of the $Fpr2^{-/-}$ mouse colony

The targeting vector (Fig. 1*A*) underwent homologous recombination in 8 out of 96 embryonic stem cell clones. Blastocyst injections were performed using two different clones, both of which produced high-quality chimaeras capable of high-frequency germline transmission. Examples of genotyping results obtained by Southern blot analysis and multiplex PCR are shown in Fig. 1*B* and Fig. 1*C*. Expression of Fpr1 was similar in cells and tissues from WT and $Fpr2^{-/-}$ mice (Fig. 1*C*). The correct expression of the transgene was confirmed by detection of GFP fluorescence in a subpopulation of blood cells and primary Mϕs (Fig. 1*D*).

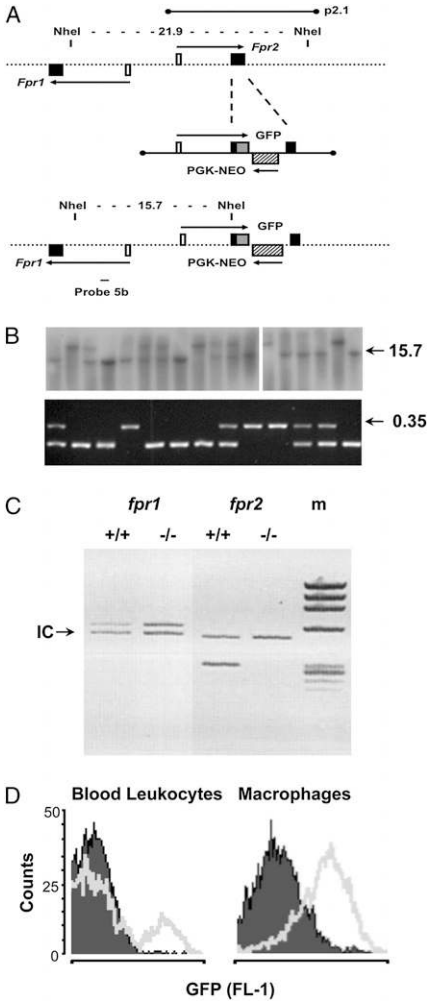

FIGURE 1. Generation of the $Fpr2^{-/-}$ mouse colony. *A*, Schematic representation of a region of ~30 kb of mouse genomic DNA spanning the *fpr1* and *fpr2* genes. The alignment of the 14.12-kb λ insert p2.1 is shown, along with the locations of the NheI restriction sites used for Southern blot screening. Filled boxes are coding exons; white boxes are noncoding exons; the hatched box represents the Pgk-neo cassette inserted in reverse orientation into the coding region of Fpr2; the gray box shows GFP fused in-frame with the ATG start codon; arrows indicate primary transcripts. *B*, Southern blot analysis (*top panel*) screening of tail clip DNA digested with the enzyme NheI. Probe 5b generates bands of 21.9 and 15.7 kb for WT and targeted alleles, respectively. Genotyping by multiplex PCR (*bottom panel*) also is reported. The F1/B11 primer pair produces a band of 233 bp using WT DNA, whereas the F1/GB4 pair gives a band of 351 bp (0.35) if the targeted allele is present. *C*, Multiplex PCR was used to compare the expression of *fpr1* and *fpr2* in WT and $Fpr2^{-/-}$ mice. Primers were compared with the internal control gene (18S rRNA) denoted by the arrow. *D*, Detection of the GFP target/reporter insert by flow cytometry. Cell samples (peripheral blood or Mϕs) from WT (opaque) or $Fpr2^{-/-}$ (transparent) mice as analyzed by flow cytometry in the FL-1 channel (representative of six or more distinct cell preparations).

Phenotype of Fpr2$^{-/-}$ cells: Agonist-dependent readouts

Radioligand binding. The validity of our transgenic strategy was assessed using [^{125}I]-labeled W-peptide, a synthetic hexapeptide that is a high-affinity ligand for Fpr2 (30). Specific binding to Mϕs was calculated in WT Mϕs by the addition of increasing concentrations of tracer (0.1–820 pmol) in the presence of a constant concentration of cold peptide (10 μM; Fig. 2*A*). The data were used to generate a Scatchard plot (Fig. 2*B*), which revealed the existence of both high- and low-affinity binding sites for W-peptide. This finding is in line with an earlier study (30). The high-affinity site had a K_d of ~44 pmol and a B_{max} of ~12 pmol.

WT Mϕs bound the tracer peptide and this was displaced by unlabeled peptide (30–3000 nM) in a concentration-dependent fashion (Fig. 2*C*). In contrast, the tracer was unable to bind to Fpr2$^{-/-}$ Mϕ cells, thus confirming deletion of the receptor.

Mϕ chemotaxis. To determine the functional relevance of the receptor knockout, we used established cellular readouts in vitro. fMLP provoked optimal Mϕ chemotaxis at 1 μM [in line with its affinity for mouse Fpr1 (31)]. At concentrations >1 μM, the effect of fMLP was partly reliant on Fpr2, because it was attenuated significantly when Mϕs were prepared from Fpr2$^{-/-}$ mice (Fig. 2*D*).

Chemotaxis was promoted consistently by SAA in WT cells (Fig. 2*E*) but absent in Fpr2$^{-/-}$ Mϕs. Both AnxA1 (data not shown) and its N-terminal–derived peptide Ac2–26 (Fig. 2*E*) were inactive as chemoattractants, but SAA-induced chemotaxis was inhibited markedly by Mϕ pretreatment with 1 μM Ac2–26 (Fig. 2*F*).

ERK phosphorylation. We chose ERK phosphorylation as a robust readout (13) to test the responsiveness of Fpr2$^{-/-}$ cells to non-chemokinetic receptor ligands. We used two selective, synthetic compounds, W-peptide (30) and a nonpeptidic molecule, Cpd43 (32), as agonists. In both cases, addition to Mϕs provoked a concentration-dependent rapid phosphorylation of ERK in WT cells (Fig. 3*A*) but not in Fpr2$^{-/-}$ Mϕs (Fig. 3*B*). Equally important, the agonistic effect of peptide Ac2–26, which is known to activate all FPRs under in vitro experimental settings (33), was abrogated in Fpr2$^{-/-}$ Mϕs (Fig. 3*C*), whereas the response elicited by SAA was retained (Fig. 3*D*).

Fpr2 pharmacology and models of acute inflammation

Treatment with hrAnxA1 produced dose-response inhibition of PMN (Gr1$^+$ cells) accumulation into murine dorsal air pouches inflamed with IL-1β, with substantial inhibition (≥70%, $p < 0.01$, $n = 10$) at a dose of 1 μg per mouse (~30 pmol; Fig. 4*A*). The inhibitory action of AnxA1 was attenuated greatly (~25–30%; NS) in Fpr2$^{-/-}$ mice. Also notable was the reduced efficacy of dexamethasone in the Fpr2$^{-/-}$ mice at a dose that significantly reduced Gr1$^+$ cell infiltrate into inflamed WT pouches (Fig. 4*A*).

The involvement of Fpr2 in the antimigratory properties of hrAnxA1 was not restricted to dorsal air pouches; when PMN trafficking was elicited by i.p. zymosan, hrAnxA1 (1 μg i.v.) significantly inhibited Gr1$^+$ cell content in 4 h peritoneal fluids (38 ± 9% reduction versus cell recruitment in the vehicle group, $n = 6$, $p < 0.05$; Fig. 4*B*) but was inactive in Fpr2$^{-/-}$ mice (−5 ± 12%, $n = 6$, NS; Fig. 4*B*). The expression of *fpr* and *anxa1* mRNA was

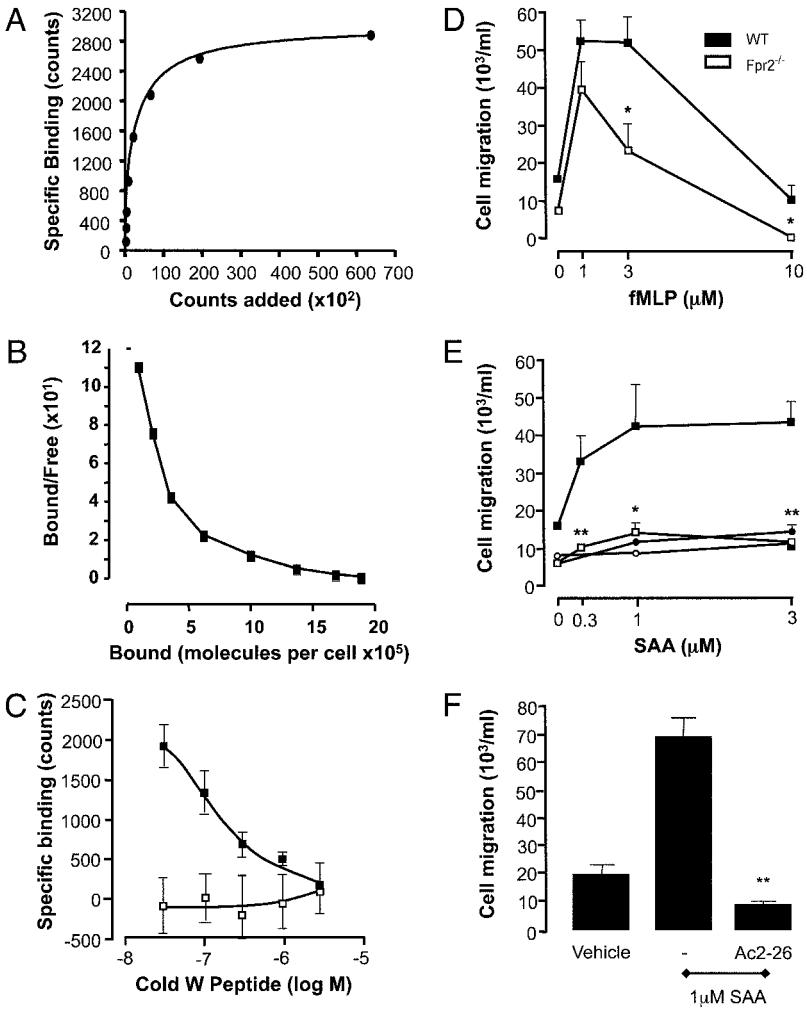

FIGURE 2. Functional deletion of Fpr2 in vitro. *A*, Specific binding of [^{125}I]-labeled W-peptide is represented as number of molecules bound compared with the γ-counts. *B*, This data allowed the calculation of a Scatchard plot. *C*, Fpr2-specific binding to WT (black) and Fpr2$^{-/-}$ (white) Mϕs was assessed by measuring the competitive displacement of the [^{125}I]-labeled W-peptide trace by cold peptide. *D* and *E*, The chemotactic responses of WT (black) and Fpr2$^{-/-}$ (white) Mϕs toward different concentrations of (*D*) fMLP, (*E*) SAA, or Ac2–26 were assessed by using 5-μm 96-well ChemoTx plates. Data are mean ± SEM of three experiments in quadruplicate. $*p < 0.05$; $**p < 0.01$, compared with respective WT Mϕ group by Student *t* test. *F*, WT Mϕs were pretreated with either vehicle or 1 μM Ac2–26 for 10 min prior to SAA-induced (1 μM) chemotaxis. $**p < 0.01$; compared with vehicle-treated group by Student *t* test ($n = 4$).

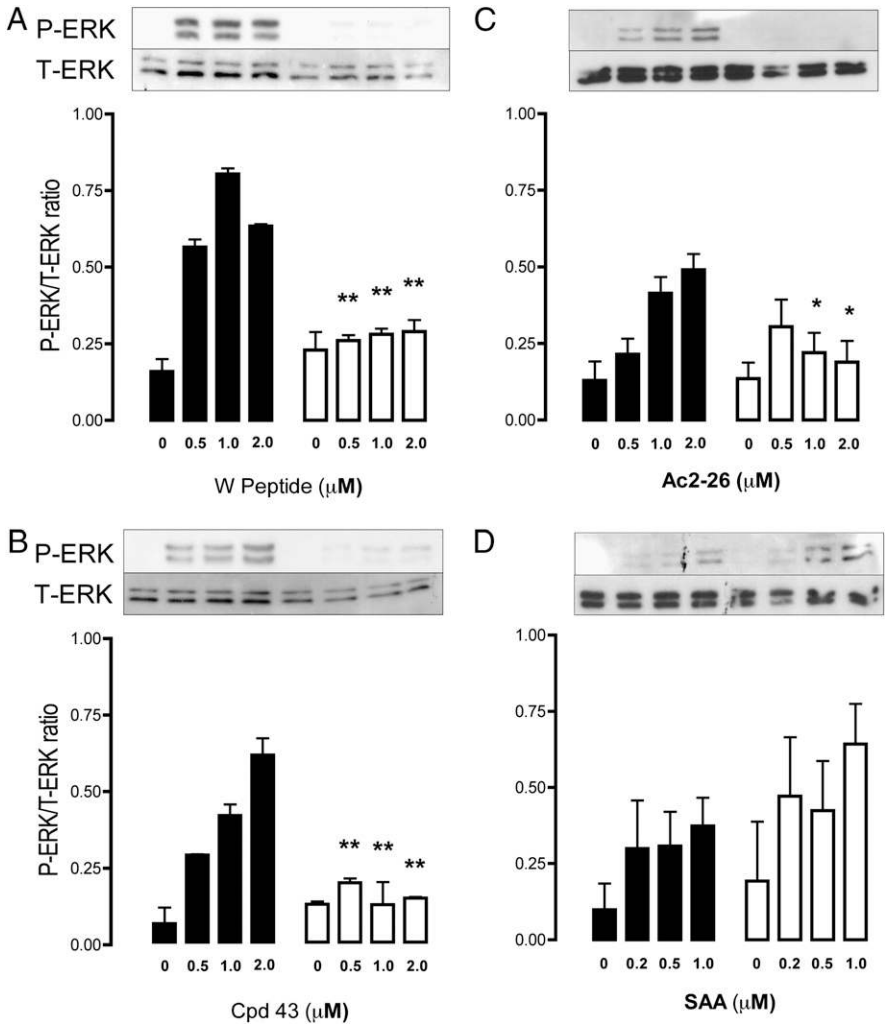

FIGURE 3. Intracellular signaling induced by Fpr2 ligation. Phosphorylation of ERK was monitored by Western blot analysis, with Mϕs exposed to a concentration range of W-peptide, Cpd43, Ac2–26, and SAA (*A–D*, respectively) for 10 min at 37°C. Representative blots are shown; respective bar histograms showing cumulative data (n = 3). Closed bars, WT Mϕs; open bars, Fpr2$^{-/-}$ Mϕs. Data, expressed as the ratio of phospho-ERK to total ERK, are mean ± SEM of three distinct experiments with different Mϕ cultures. $*p < 0.05$; $**p < 0.01$; compared with respective WT Mϕs by Mann-Whitney U test.

similar in both WT and Fpr2$^{-/-}$ peritoneal cells, under resting or acute inflammatory conditions (data not shown).

We tested a number of structurally disparate FPR2/ALX ligands in the mouse air-pouch system following i.v. administration. Fig. 4*C* reports this data with doses presented in molar terms to facilitate quantitative comparison (the effects measured with hrAnxA1 are shown for comparative purposes). Peptide Ac2–26 dose-dependently inhibited (30–50%) Gr1$^+$ cell recruitment promoted by IL-1β, an effect absent in Fpr2$^{-/-}$ mice. At anti-inflammatory doses (15, 32), LXA_4 and Cpd43 produced 50–75% inhibition of cell recruitment (n = 6, $p < 0.01$ in both cases) in WT mice but were ineffective in Fpr2$^{-/-}$ animals. Intriguingly, SAA provoked a marked increase in the number of cells recruited by IL-1β (1.5-fold over control values of 3.0 ± 0.4 × 10^6 per cavity); again this effect was mediated through Fpr2 because the Fpr2$^{-/-}$ mice did not share this response (Fig. 4*C*).

Physiological role of Fpr2 in inflammation

Because we did not observe differences in the leukocyte trafficking responses upon stimulation with IL-1β or zymosan between genotypes, we compared the mouse colonies applying either protocol shown to be sensitive to Fpr2 agonists AnxA1 and LXA_4 (28, 34) or more complex models of inflammation. An ischemia–reperfusion insult provoked interaction between circulating leukocytes and postcapillary venules of the mesenteric vascular bed, quantified both at 45 and 90 min postreperfusion (Fig 5*A*, 5*B*). Deletion of Fpr2 caused a discrete alteration in these responses, with a significant increase above WT values only for the degree of cell emigration (Fig. 5*A*). In contrast, longer reperfusion times unveiled an important protective function for Fpr2, because a marked increase ($p < 0.01$) in adherent and emigrated cells was measured in Fpr2$^{-/-}$ mice (Fig. 5*B*). Representative images depicting these vascular differences at 90 min postreperfusion are shown in Fig. 5*C*.

The enhanced acute inflammatory phenotype of the Fpr2$^{-/-}$ mouse emerged further using the carrageenan-induced paw edema model. There was a significant increase in paw swelling in Fpr2$^{-/-}$ mice compared with that in WT animals, significant as early as 4 h after carrageenan administration (~2.5-fold increase) and stable at peak response (8 h time point; +60% in Fpr2$^{-/-}$ mice) (Fig. 6*A*). Histological analyses of paws collected at the 4 h time point revealed larger numbers of infiltrating leukocytes in the dorsal areas of the paws (Fig. 6*B*) in the Fpr2$^{-/-}$ mice.

Administration of K/B × N serum provokes a rapid arthrogenic response mediated by cells of the innate immune system (35). Though reaching a maximum at day 7 in both strains, we noted a striking exacerbation and prolongation of the disease in Fpr2$^{-/-}$ mice (Fig. 6*C*, 6*D*, respectively), such that symptoms were still evident at day 18, when the response had subsided in WT mice (Fig. 6*C*). To our knowledge, this is the first data highlighting the tonic inhibitory action mediated through Fpr2 in a model of chronic pathology. A marked upregulation of *fpr2* gene expression (as well as *fpr* and *anxa1*) was detected in the inflamed joints during the course of the arthritic response (data not shown).

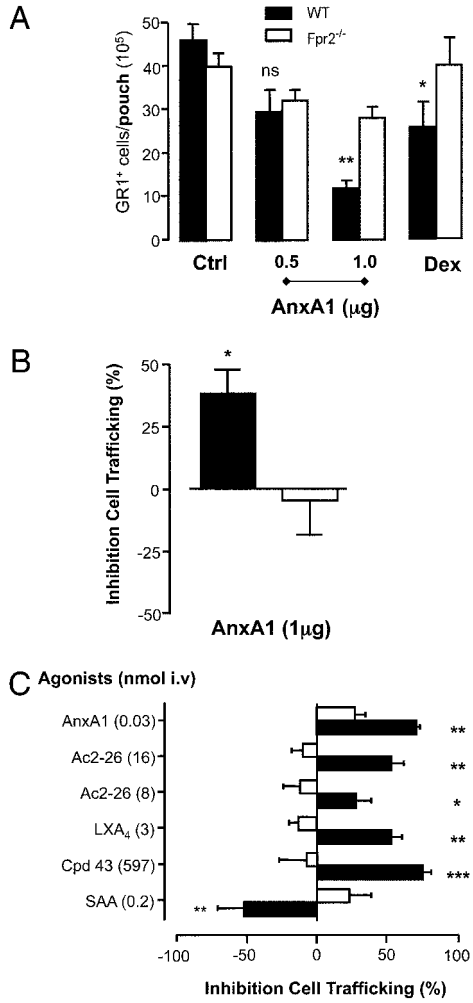

FIGURE 4. AnxA1 and other Fpr2 ligands in the air-pouch and zymosan peritonitis model. *A*, AnxA1 (given −10 min) or dexamethasone (0.5 mg/kg, given −1 h) were administered i.v. prior to IL-1β (20 ng) injection into 6-d-old air pouches in WT (closed bars) and Fpr2$^{-/-}$ mice (open bars). $*p < 0.05$; $**p < 0.01$, significant differences between treated and untreated WT values. There was no significant difference between the values for Fpr2$^{-/-}$ mice with any treatment (ANOVA). *B*, AnxA1 (1 μg, given −10 min) was administered i.v. prior to zymosan (1 mg, i.p.) injection. Gr1$^+$ cell influx into the air pouch or peritoneal cavity was quantified at the 4 h time point by cell counting and flow cytometry. *C*, Fpr2 ligands were given i.v. at the doses shown (nanomoles) with data being reported as percentage of inhibition compared with vehicle-treated mice. The IL-1β response was similar in WT and Fpr2$^{-/-}$ mice (~3×10^6 cells per pouch). $*p < 0.05$; $**p < 0.01$; $***p < 0.001$; compared with respective control values (original numbers) by Student *t* test. In all of the cases, data are mean ± SEM of 6–12 mice per group.

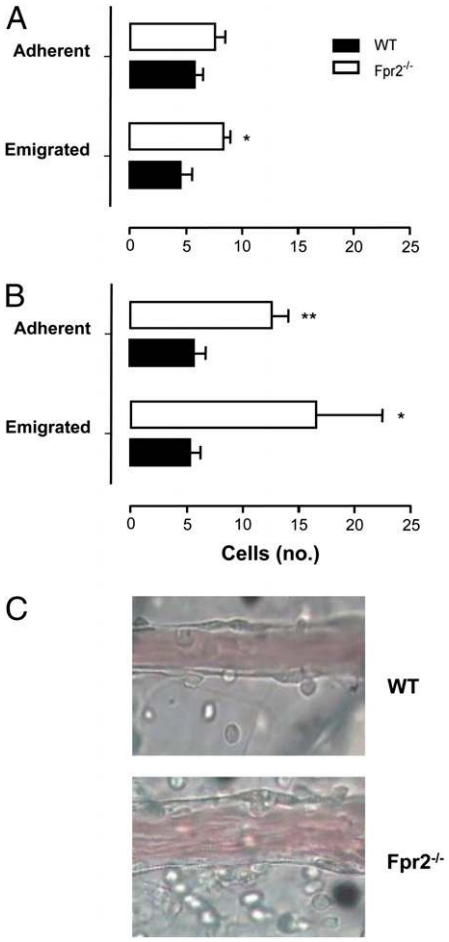

FIGURE 5. Mesenteric ischemia–reperfusion injury of WT and Fpr2$^{-/-}$ mice. *A* and *B*, Mesenteric circulation was subjected to 30 min ischemia followed by (*A*) 45 or (*B*) 90 min perfusion. *C*, A representative field analyzed following 90 min perfusion. WT and Fpr2$^{-/-}$ mice, spanning 100 μm in length and surrounding 50 μm of tissue either side of the vessel wall. Data are mean ± SEM of three fields per mouse of $n = 5$ mice per group. $**p < 0.01$; $*p < 0.05$; compared with WT by Student *t* test.

Discussion

We have generated a new colony of mice in which the gene for Fpr2 has been deleted and have used this model to investigate the pathophysiology and pharmacology of this receptor in both cell-based assays and complex models in vivo. In the mouse, the *fpr* gene cluster (on chromosome 17) has undergone differential expansion, and at least eight genes have been identified (12, 20). Two of these do not appear to be expressed, and another is seen only in the skeletal muscle. Three genes (*fpr1*, *fpr2*, and *fpr-rs3*) are expressed in leukocytes, spleen, and lung.

To confirm that deletion of the *fpr2* gene was responsible for the transcription of the functional equivalent of human FPR2/ALX, we conducted radioligand binding assays using [^{125}I]WKYMVm. The absence of binding in Fpr2$^{-/-}$ Mϕs even at high concentrations reflected the specificity of our transgenic technique and revealed a lack of functional compensation by Fpr1 binding.

The absence of Fpr2 had little observable effect on the phenotype under naive conditions. Healthy litters were produced with the expected Mendelian ratio, and mice grew normally with no apparent adverse effects, spontaneous infections, or weight gain. The assessment of generic Ag markers and proportions of circulating immune cells were unaffected, with observations matching those made in the Fpr1$^{-/-}$ colony (31).

The results of the chemotaxis assays present significant parallels with a previous study assessing the migration of transfected HEK-293/Fpr2 toward these ligands (36). This profile is in line with the actions of fMLP at its low-affinity receptor (21). Our data furthermore indicate an exclusive role of Fpr2 in SAA-induced locomotion of human and mouse PMNs and monocytes (13, 22). Because Ac2–26 markedly inhibited SAA-mediated chemotaxis, although unable to induce Mϕ locomotion by itself, these data provide the first hint that murine Fpr2 can integrate two counter-regulatory pathways.

To validate the ligand specificity of this GPCR, we used phosphorylation of ERK (37), a well-established signaling pathway associated with the FPR family (12). W-peptide, a synthetic hexapeptide with a good degree of specificity for Fpr2, induced

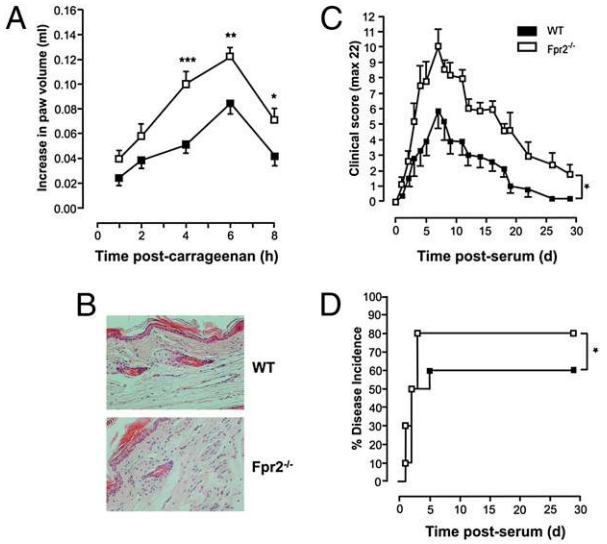

FIGURE 6. Carrageenan-induced paw edema and passive serum-induced arthritis: exacerbation in Fpr2$^{-/-}$ mice. Mice paws were injected with 50 μl 1% carrageenan solution. *A*, Time course of the paw swelling in WT and Fpr2$^{-/-}$ mice. Data are shown as mean ± SEM of $n = 15$ animals. $*p < 0.05$; $**p < 0.01$; $***p < 0.001$; Student *t* test. *B*, Histological analysis in dorsal section of paws at 4 h time point. Mice received 200 μl i.p. of arthrogenic K/B × N serum. *C*, Time course of the clinical arthritic score in WT and Fpr2$^{-/-}$ mice. Data are mean ± SEM of $n = 6$ mice. $*p < 0.05$; two-way ANOVA. *D*, Percentage disease incidence (cut-off score ≥3). $*p < 0.05$; log-rank test.

a concentration-dependent response that was absent in Fpr2$^{-/-}$ Mϕs, supporting the validity of our transgenic strategy. Furthermore, a selective nonpeptidic FPR2/ALX agonist with anti-inflammatory effects, Cpd43 (32), promoted an ERK response in Mϕs that was also dependent on Fpr2. Altogether, these data suggest the homology between the human and the mouse receptors translates into functional similarities. Interestingly, the ERK response to SAA was not diminished in Fpr2$^{-/-}$ Mϕs, a finding in line with the notion that this protein activates multiple receptors and that FPR2/ALX is not solely responsible for intracellular phospho-ERK generation (13, 38, 39). Collectively, these experiments indicate that we have generated a viable mouse colony deficient in Fpr2 (the orthologue of human FPR2/ALX) and that initial characterizations, at the cellular level, were congruent with the current understanding of the biology of the agonists used (20). Furthermore, because peptide Ac2–26- and Cpd43-induced phospho-ERK responses in Mϕs evidently rely upon Fpr2, we could test confidently the impact that *fpr2* deletion had on experimental inflammation.

PMN recruitment is a hallmark of the inflammatory response (1, 40). It is exquisitely susceptible to inhibition by endogenous anti-inflammatory pathways (41), including the FPR2/ALX agonists LXA_4 (8) and AnxA1 (9). To investigate the role of Fpr2 in orchestrating acute-phase inflammation, a number of Fpr2 ligands were assessed for their abilities to control leukocyte recruitment triggered by IL-1β as an example of a receptor-independent stimulus.

AnxA1 is established as a potent endogenous anti-inflammatory protein mediating a number of antimigratory and proresolving actions in vitro and in vivo (10). The antimigratory action of hrAnxA1 was attenuated largely in Fpr2$^{-/-}$ mice, suggesting that its influence on PMN recruitment depends largely upon Fpr2. This finding is in line with the fact that a high proportion of the antimigratory action of hrAnxA1 is retained in *fpr1*$^{-/-}$ mice (42). Dexamethasone, which releases AnxA1 from PMNs within minutes (9), was ineffective in Fpr2$^{-/-}$ mice. Whereas it is clear that the anti-inflammatory properties of glucocorticoids result from multiple molecular and cellular mechanisms (43), a functional link with AnxA1 is confirmed by their reduced efficacy in AnxA1-deficient mice (e.g., Refs. 7, 44). Glucocorticoids can upregulate FPR2/ALX gene and protein expression in human cells (45) and in experimental dermatitis (46). A similar phenomenon also is seen in the case of FPR (47). These intriguing results beg the question of the role of this GPCR in the overall anti-inflammatory and multiple cellular effects of glucocorticoids (43). More experiments are required to elucidate these initial observations, though it is likely that Fpr2 (or FPR2/ALX in human) upregulation by glucocorticoids may mediate a permissive action in the context of inflammatory resolution (5). Furthermore, the diversity of reports on *FPR2/ALX* versus *FPR* gene induction might also indicate that distinct glucocorticoids produce different, cell-specific outcomes and gene expression profiles (47).

With the air-pouch model, novel results were seen when multiple Fpr2 ligands were tested. For instance, Cpd43, peptide Ac2–26, and LXA_4 all reduced PMN migration selectively in WT mice but not in Fpr2 null animals. To the contrary, SAA increased PMN recruitment, an effect again absent in Fpr2$^{-/-}$ mice. This is the first demonstration that a single GPCR can mediate opposing effects of SAA and other ligands in vivo, a feature reported in some in vitro systems (e.g., Refs. 13, 48). Furthermore, whereas the biology of SAA is complex and its receptors uncertain (49), our study indicates conclusively that stimulation of cell locomotion by SAA in vitro and in vivo requires Fpr2. Finally, from these data, it is also clear that this receptor, and most likely its human counterpart FPR2/ALX, is an ideal model for testing ligand-biased responses and, possibly, ligand-specific receptor homo- or heterodimerization (50). In this respect, it is interesting to note that human FPR2/ALX can form heterodimers with the leukotriene B_4 receptor, at least in artificial cell systems (51).

In the last part of the study, we investigated the pathophysiological roles of Fpr2, noting that in the acute models of cell recruitment to specific cavities no differences emerged between WT and Fpr2$^{-/-}$ mice. Because both AnxA1 and LXA_4 exert exquisite effects in the inflamed microcirculation, with particular efficacy against ischemia–reperfusion insults (inflammation from within) (34, 52, 53), we compared responses postreperfusion in the mesenteric microcirculation. A protective role for Fpr2 was evident, and it followed a time-dependent profile, so that much higher degrees of cell adhesion and emigration could be measured at 90 min postreperfusion. These observations have the implicit caveats that Fpr2 agonists must be present or produced in this early phase of vascular inflammation. Indeed, we propose endogenous AnxA1 to be externalized on the cell surfaces of adherent PMNs (54), promoting detachment (28, 55). Furthermore, concentrations of LXA_4 in localized tissue have been shown to be rapidly enhanced following ischemia–reperfusion injury (56). Finally, it should be noted that augmented degrees of cell adhesion and emigration also have been reported in microvascular beds of AnxA1$^{-/-}$ mice (7, 57) but not in Fpr1$^{-/-}$ animals (58), making a strong functional parallel between two elements (ligand and receptor) of the AnxA1 pathway (9).

The same thinking underlies the experiments of paw edema, a model where AnxA1$^{-/-}$ mice displayed higher inflammatory responses (44). Fpr2$^{-/-}$ mice had a much more rapid, and higher, edema responses in the paw compared with those of WT controls, and this was associated with a marked influx of blood-borne leukocytes in its dorsal tissues. It is unclear why these differences in cell influx were evident in this model and not in IL-1β–induced

air-pouch or zymosan peritonitis assays; it is likely that in these cavities other processes may take place, including cell efflux or cell death (10), which is not reflected by the paw inflammation model, where a strong inflammatory response is localized in a discrete tissue site. Furthermore, it cannot be excluded that the different stimulus may have an impact, with the response to carrageenan being mediated, for instance, by a variety of processes, steps, or mediators (59). However, this explanation could be acceptable for IL-1β and carrageenan, because they are very different stimuli (with the cytokine promoting selective leukocyte recruitment without overt inflammatory responses), but not for zymosan and carrageenan, because both stimuli are nonsoluble and nonspecific. Further studies would be required to explain these apparent discrepancies.

The anti-inflammatory nature of Fpr2, evident in the carrageenan paw edema model, emerged more strongly in a longer-lasting model of inflammation caused by the K/B × N serum. Injection of this serum promotes a rapid arthritic response lasting up to 28 d (depending on the volume injected). The etiology of the disease relies mainly upon PMN, Mϕ, and mast cell activation (35, 60). Greater acute inflammation and a prolongation of inflammatory arthritis were observed in $Fpr2^{-/-}$ mice, with a higher penetrance of severe symptoms, corroborating the overall anti-inflammatory role of this GPCR. The K/B × N serum arthritis model already has been used to extend mechanistic observations generated with models of acute inflammation to settings modeling inflammatory arthritis (29, 61) and proved ideal for determining the potential anti-inflammatory functions of Fpr2. We would propose a model whereby, in the absence of the tonic inhibitory influence of Fpr2 (likely to be induced by AnxA1 and LXA_4), greater activation of joint Mϕs and mast cells, will lead to a more pronounced accumulation of PMNs, leading ultimately to the more pronounced and prolonged arthritic response observed in $Fpr2^{-/-}$ mice. Not many studies have applied this model to other elements of this endogenous anti-inflammatory pathway, one exception being the recent study by Krönke et al. (62). These authors have applied this model to mice deficient for both 12- and 15-lipoxygenase, enzymes required for the synthesis of LXA_4, observing exacerbated inflammatory arthritis associated with lower joint levels of this anti-inflammatory lipid.

In conclusion, we describe for the first time, the functions of Fpr2 in experimental models of inflammation. Not only does this receptor transduce inhibitory signals from endogenous effectors of anti-inflammation (AnxA1 and LXA_4) as well as new chemical entities such as Cpd43, but it also regulates other aspects of the host inflammatory reaction including leukocyte interaction with postcapillary venules, tissue edema, and joint arthritis. Our data point to the existence of subtle, yet reproducible, modulatory loops centered on Fpr2 and its ligands and provide a compelling rationale for developing novel anti-inflammatory therapeutics based upon on agonists of Fpr2 and its human counterpart FPR2/ALX (32, 63).

Disclosures

The authors have no financial conflicts of interest.

References

1. Nathan, C. 2002. Points of control in inflammation. *Nature* 420: 846–852.
2. Serhan, C. N., and J. Savill. 2005. Resolution of inflammation: the beginning programs the end. *Nat. Immunol.* 6: 1191–1197.
3. Luster, A. D., R. Alon, and U. H. von Andrian. 2005. Immune cell migration in inflammation: present and future therapeutic targets. *Nat. Immunol.* 6: 1182–1190.
4. Serhan, C. N. 2007. Resolution phase of inflammation: novel endogenous anti-inflammatory and proresolving lipid mediators and pathways. *Annu. Rev. Immunol.* 25: 101–137.
5. Serhan, C. N., S. D. Brain, C. D. Buckley, D. W. Gilroy, C. Haslett, L. A. O'Neill, M. Perretti, A. G. Rossi, and J. L. Wallace. 2007. Resolution of inflammation: state of the art, definitions and terms. *FASEB J.* 21: 325–332.
6. Bannenberg, G. L., N. Chiang, A. Ariel, M. Arita, E. Tjonahen, K. H. Gotlinger, S. Hong, and C. N. Serhan. 2005. Molecular circuits of resolution: formation and actions of resolvins and protectins. *J. Immunol.* 174: 4345–4355.
7. Damazo, A. S., S. Yona, R. J. Flower, M. Perretti, and S. M. Oliani. 2006. Spatial and temporal profiles for anti-inflammatory gene expression in leukocytes during a resolving model of peritonitis. *J. Immunol.* 176: 4410–4418.
8. Chiang, N., C. N. Serhan, S. E. Dahlén, J. M. Drazen, D. W. Hay, G. E. Rovati, T. Shimizu, T. Yokomizo, and C. Brink. 2006. The lipoxin receptor ALX: potent ligand-specific and stereoselective actions in vivo. *Pharmacol. Rev.* 58: 463–487.
9. Perretti, M., and F. D'Acquisto. 2009. Annexin A1 and glucocorticoids as effectors of the resolution of inflammation. *Nat. Rev. Immunol.* 9: 62–70.
10. Schwab, J. M., N. Chiang, M. Arita, and C. N. Serhan. 2007. Resolvin E1 and protectin D1 activate inflammation-resolution programmes. *Nature* 447: 869–874.
11. Perretti, M., N. Chiang, M. La, I. M. Fierro, S. Marullo, S. J. Getting, E. Solito, and C. N. Serhan. 2002. Endogenous lipid- and peptide-derived anti-inflammatory pathways generated with glucocorticoid and aspirin treatment activate the lipoxin A_4 receptor. *Nat. Med.* 8: 1296–1302.
12. Ye, R. D., F. Boulay, J. M. Wang, C. Dahlgren, C. Gerard, M. Parmentier, C. N. Serhan, and P. M. Murphy. 2009. International Union of Basic and Clinical Pharmacology. LXXIII. Nomenclature for the formyl peptide receptor (FPR) family. *Pharmacol. Rev.* 61: 119–161.
13. He, R., H. Sang, and R. D. Ye. 2003. Serum amyloid A induces IL-8 secretion through a G protein-coupled receptor, FPRL1/LXA4R. *Blood* 101: 1572–1581.
14. Babbin, B. A., W. Y. Lee, C. A. Parkos, L. M. Winfree, A. Akyildiz, M. Perretti, and A. Nusrat. 2006. Annexin I regulates SKCO-15 cell invasion by signaling through formyl peptide receptors. *J. Biol. Chem.* 281: 19588–19599.
15. Chiang, N., I. M. Fierro, K. Gronert, and C. N. Serhan. 2000. Activation of lipoxin $A_{(4)}$ receptors by aspirin-triggered lipoxins and select peptides evokes ligand-specific responses in inflammation. *J. Exp. Med.* 191: 1197–1208.
16. Ying, G., P. Iribarren, Y. Zhou, W. Gong, N. Zhang, Z. X. Yu, Y. Le, Y. Cui, and J. M. Wang. 2004. Humanin, a newly identified neuroprotective factor, uses the G protein-coupled formylpeptide receptor-like-1 as a functional receptor. *J. Immunol.* 172: 7078–7085.
17. Le, Y., W. Gong, H. L. Tiffany, A. Tumanov, S. Nedospasov, W. Shen, N. M. Dunlop, J. L. Gao, P. M. Murphy, J. J. Oppenheim, and J. M. Wang. 2001. Amyloid β42 activates a G-protein-coupled chemoattractant receptor, FPR-like-1. *J. Neurosci.* 21: RC123.
18. Resnati, M., I. Pallavicini, J. M. Wang, J. Oppenheim, C. N. Serhan, M. Romano, and F. Blasi. 2002. The fibrinolytic receptor for urokinase activates the G protein-coupled chemotactic receptor FPRL1/LXA_4R. *Proc. Natl. Acad. Sci. USA* 99: 1359–1364.
19. Le, Y., R. D. Ye, W. Gong, J. Li, P. Iribarren, and J. M. Wang. 2005. Identification of functional domains in the formyl peptide receptor-like 1 for agonist-induced cell chemotaxis. *FEBS J.* 272: 769–778.
20. Le, Y., P. M. Murphy, and J. M. Wang. 2002. Formyl-peptide receptors revisited. *Trends Immunol.* 23: 541–548.
21. Hartt, J. K., G. Barish, P. M. Murphy, and J. L. Gao. 1999. *N*-Formylpeptides induce two distinct concentration optima for mouse neutrophil chemotaxis by differential interaction with two *N*-formylpeptide receptor (FPR) subtypes. Molecular characterization of FPR2, a second mouse neutrophil FPR. *J. Exp. Med.* 190: 741–747.
22. Su, S. B., W. Gong, J. L. Gao, W. Shen, P. M. Murphy, J. J. Oppenheim, and J. M. Wang. 1999. A seven-transmembrane, G protein-coupled receptor, FPRL1, mediates the chemotactic activity of serum amyloid A for human phagocytic cells. *J. Exp. Med.* 189: 395–402.
23. Vaughn, M. W., R. J. Proske, and D. L. Haviland. 2002. Identification, cloning, and functional characterization of a murine lipoxin A4 receptor homologue gene. *J. Immunol.* 169: 3363–3369.
24. Hayhoe, R. P., A. M. Kamal, E. Solito, R. J. Flower, D. Cooper, and M. Perretti. 2006. Annexin 1 and its bioactive peptide inhibit neutrophil-endothelium interactions under flow: indication of distinct receptor involvement. *Blood* 107: 2123–2130.
25. Perretti, M., and R. J. Flower. 1993. Modulation of IL-1-induced neutrophil migration by dexamethasone and lipocortin 1. *J. Immunol.* 150: 992–999.
26. Perretti, M., E. Solito, and L. Parente. 1992. Evidence that endogenous interleukin-1 is involved in leukocyte migration in acute experimental inflammation in rats and mice. *Agents Actions* 35: 71–78.
27. Henriques, M. G., P. M. Silva, M. A. Martins, C. A. Flores, F. Q. Cunha, J. Assreuy-Filho, and R. S. Cordeiro. 1987. Mouse paw edema. A new model for inflammation? *Braz. J. Med. Biol. Res.* 20: 243–249.
28. Gavins, F. N., S. Yona, A. M. Kamal, R. J. Flower, and M. Perretti. 2003. Leukocyte antiadhesive actions of annexin 1: ALXR- and FPR-related anti-inflammatory mechanisms. *Blood* 101: 4140–4147.
29. Rossi, A. G., D. A. Sawatzky, A. Walker, C. Ward, T. A. Sheldrake, N. A. Riley, A. Caldicott, M. Martinez-Losa, T. R. Walker, R. Duffin, et al. 2006. Cyclin-dependent kinase inhibitors enhance the resolution of inflammation by promoting inflammatory cell apoptosis. *Nat. Med.* 12: 1056–1064.
30. Le, Y., W. Gong, B. Li, N. M. Dunlop, W. Shen, S. B. Su, R. D. Ye, and J. M. Wang. 1999. Utilization of two seven-transmembrane, G protein-coupled receptors, formyl peptide receptor-like 1 and formyl peptide receptor, by the synthetic hexapeptide WKYMVm for human phagocyte activation. *J. Immunol.* 163: 6777–6784.
31. Gao, J. L., E. J. Lee, and P. M. Murphy. 1999. Impaired antibacterial host defense in mice lacking the *N*-formylpeptide receptor. *J. Exp. Med.* 189: 657–662.

32. Bürli, R. W., H. Xu, X. Zou, K. Muller, J. Golden, M. Frohn, M. Adlam, M. H. Plant, M. Wong, M. McElvain, et al. 2006. Potent hFPRL1 (ALXR) agonists as potential anti-inflammatory agents. *Bioorg. Med. Chem. Lett.* 16: 3713–3718.
33. Ernst, S., C. Lange, A. Wilbers, V. Goebeler, V. Gerke, and U. Rescher. 2004. An annexin 1 N-terminal peptide activates leukocytes by triggering different members of the formyl peptide receptor family. *J. Immunol.* 172: 7669–7676.
34. Scalia, R., J. Gefen, N. A. Petasis, C. N. Serhan, and A. M. Lefer. 1997. Lipoxin A_4 stable analogs inhibit leukocyte rolling and adherence in the rat mesenteric microvasculature: role of P-selectin. *Proc. Natl. Acad. Sci. USA* 94: 9967–9972.
35. Ji, H., K. Ohmura, U. Mahmood, D. M. Lee, F. M. Hofhuis, S. A. Boackle, K. Takahashi, V. M. Holers, M. Walport, C. Gerard, et al. 2002. Arthritis critically dependent on innate immune system players. *Immunity* 16: 157–168.
36. Liang, T. S., J. M. Wang, P. M. Murphy, and J. L. Gao. 2000. Serum amyloid A is a chemotactic agonist at FPR2, a low-affinity *N*-formylpeptide receptor on mouse neutrophils. *Biochem. Biophys. Res. Commun.* 270: 331–335.
37. Gripentrog, J. M., and H. M. Miettinen. 2008. Formyl peptide receptor-mediated ERK1/2 activation occurs through G_i and is not dependent on β-arrestin1/2. *Cell. Signal.* 20: 424–431.
38. Baranova, I. N., T. G. Vishnyakova, A. V. Bocharov, R. Kurlander, Z. Chen, M. L. Kimelman, A. T. Remaley, G. Csako, F. Thomas, T. L. Eggerman, and A. P. Patterson. 2005. Serum amyloid A binding to CLA-1 (CD36 and LIMPII analogous-1) mediates serum amyloid A protein-induced activation of ERK1/2 and p38 mitogen-activated protein kinases. *J. Biol. Chem.* 280: 8031–8040.
39. He, R. L., J. Zhou, C. Z. Hanson, J. Chen, N. Cheng, and R. D. Ye. 2009. Serum amyloid A induces G-CSF expression and neutrophilia via Toll-like receptor 2. *Blood* 113: 429–437.
40. Nathan, C. 2006. Neutrophils and immunity: challenges and opportunities. *Nat. Rev. Immunol.* 6: 173–182.
41. Perretti, M. 1997. Endogenous mediators that inhibit the leukocyte-endothelium interaction. *Trends Pharmacol. Sci.* 18: 418–425.
42. Perretti, M., S. J. Getting, E. Solito, P. M. Murphy, and J. L. Gao. 2001. Involvement of the receptor for formylated peptides in the in vivo anti-migratory actions of annexin 1 and its mimetics. *Am. J. Pathol.* 158: 1969–1973.
43. Clark, A. R. 2007. Anti-inflammatory functions of glucocorticoid-induced genes. *Mol. Cell. Endocrinol.* 275: 79–97.
44. Hannon, R., J. D. Croxtall, S. J. Getting, F. Roviezzo, S. Yona, M. J. Paul-Clark, F. N. Gavins, M. Perretti, J. F. Morris, J. C. Buckingham, and R. J. Flower. 2003. Aberrant inflammation and resistance to glucocorticoids in annexin $1^{-/-}$ mouse. *FASEB J.* 17: 253–255.
45. Sawmynaden, P., and M. Perretti. 2006. Glucocorticoid upregulation of the annexin-A1 receptor in leukocytes. *Biochem. Biophys. Res. Commun.* 349: 1351–1355.
46. Hashimoto, A., Y. Murakami, H. Kitasato, I. Hayashi, and H. Endo. 2007. Glucocorticoids co-interact with lipoxin A_4 via lipoxin A_4 receptor (ALX) up-regulation. *Biomed. Pharmacother.* 61: 81–85.
47. Ehrchen, J., L. Steinmüller, K. Barczyk, K. Tenbrock, W. Nacken, M. Eisenacher, U. Nordhues, C. Sorg, C. Sunderkötter, and J. Roth. 2007. Glucocorticoids induce differentiation of a specifically activated, anti-inflammatory subtype of human monocytes. *Blood* 109: 1265–1274.
48. El Kebir, D., L. József, and J. G. Filep. 2008. Opposing regulation of neutrophil apoptosis through the formyl peptide receptor-like 1/lipoxin A_4 receptor: implications for resolution of inflammation. *J. Leukoc. Biol.* 84: 600–606.
49. Shah, C., R. Hari-Dass, and J. G. Raynes. 2006. Serum amyloid A is an innate immune opsonin for Gram-negative bacteria. *Blood* 108: 1751–1757.
50. Bosier, B., and E. Hermans. 2007. Versatility of GPCR recognition by drugs: from biological implications to therapeutic relevance. *Trends Pharmacol. Sci.* 28: 438–446.
51. Damian, M., S. Mary, A. Martin, J. P. Pin, and J. L. Banères. 2008. G protein activation by the leukotriene B_4 receptor dimer. Evidence for an absence of trans-activation. *J. Biol. Chem.* 283: 21084–21092.
52. Gavins, F. N., J. Dalli, R. J. Flower, D. N. Granger, and M. Perretti. 2007. Activation of the annexin 1 counter-regulatory circuit affords protection in the mouse brain microcirculation. *FASEB J.* 21: 1751–1758.
53. Chiang, N., K. Gronert, C. B. Clish, J. A. O'Brien, M. W. Freeman, and C. N. Serhan. 1999. Leukotriene B_4 receptor transgenic mice reveal novel protective roles for lipoxins and aspirin-triggered lipoxins in reperfusion. *J. Clin. Invest.* 104: 309–316.
54. Perretti, M., J. D. Croxtall, S. K. Wheller, N. J. Goulding, R. Hannon, and R. J. Flower. 1996. Mobilizing lipocortin 1 in adherent human leukocytes downregulates their transmigration. *Nat. Med.* 22: 1259–1262.
55. Lim, L. H., E. Solito, F. Russo-Marie, R. J. Flower, and M. Perretti. 1998. Promoting detachment of neutrophils adherent to murine postcapillary venules to control inflammation: effect of lipocortin 1. *Proc. Natl. Acad. Sci. USA* 95: 14535–14539.
56. Souza, D. G., C. T. Fagundes, F. A. Amaral, D. Cisalpino, L. P. Sousa, A. T. Vieira, V. Pinho, J. R. Nicoli, L. Q. Vieira, I. M. Fierro, and M. M. Teixeira. 2007. The required role of endogenously produced lipoxin A_4 and annexin-1 for the production of IL-10 and inflammatory hyporesponsiveness in mice. *J. Immunol.* 179: 8533–8543.
57. Chatterjee, B. E., S. Yona, G. Rosignoli, R. E. Young, S. Nourshargh, R. J. Flower, and M. Perretti. 2005. Annexin 1-deficient neutrophils exhibit enhanced transmigration in vivo and increased responsiveness in vitro. *J. Leukoc. Biol.* 78: 639–646.
58. Gavins, F. N., A. M. Kamal, M. D'Amico, S. M. Oliani, and M. Perretti. 2005. Formyl-peptide receptor is not involved in the protection afforded by annexin 1 in murine acute myocardial infarct. *FASEB J.* 19: 100–102.
59. Vinegar, R., J. F. Truax, J. L. Selph, P. R. Johnston, A. L. Venable, and K. K. McKenzie. 1987. Pathway to carrageenan-induced inflammation in the hind limb of the rat. *Fed. Proc.* 46: 118–126.
60. Lee, D. M., D. S. Friend, M. F. Gurish, C. Benoist, D. Mathis, and M. B. Brenner. 2002. Mast cells: a cellular link between autoantibodies and inflammatory arthritis. *Science* 297: 1689–1692.
61. Gray, M., K. Miles, D. Salter, D. Gray, and J. Savill. 2007. Apoptotic cells protect mice from autoimmune inflammation by the induction of regulatory B cells. *Proc. Natl. Acad. Sci. USA* 104: 14080–14085.
62. Krönke, G., J. Katzenbeisser, S. Uderhardt, M. M. Zaiss, C. Scholtysek, G. Schabbauer, A. Zarbock, M. I. Koenders, R. Axmann, J. Zwerina, et al. 2009. 12/15-Lipoxygenase counteracts inflammation and tissue damage in arthritis. *J. Immunol.* 183: 3383–3389.
63. Hecht, I., J. Rong, A. L. Sampaio, C. Hermesh, C. Rutledge, R. Shemesh, A. Toporik, M. Beiman, L. Dassa, H. Niv, et al. 2009. A novel peptide agonist of formyl-peptide receptor-like 1 (ALX) displays anti-inflammatory and cardioprotective effects. *J. Pharmacol. Exp. Ther.* 328: 426–434.

Corrections

Dufton, N., R. Hannon, V. Brancaleone, J. Dalli, H. B. Patel, M. Gray, F. D'Acquisto, J. C. Buckingham, M. Perretti, and R. J. Flower. 2010. Anti-inflammatory role of the murine formyl-peptide receptor 2: ligand-specific effects on leukocyte responses and experimental inflammation. *J. Immunol.* 184: 2611–2619.

Two papers appeared in the *Journal of Immunology* in 2010 describing the generation and use of novel transgenic mouse strains to elucidate the regulatory role of the murine, G-protein–coupled receptor mFpr2 in various aspects of the immune response (1, 2).

The paper from our laboratory (1) detailed the role for this receptor in mediating the endogenous anti-inflammatory effects of the protein annexin A1 (Anx-A1). A further paper using a different transgenic strain described experiments suggesting that the same receptor was crucial in facilitating normal innate and adaptive immune responses (2). We now write to clarify the nature of the gene deletion produced using our strategy, in the light of our latest understanding of the mouse Fpr gene family; in addition to deleting the murine Fpr2 gene, we now believe that our targeting construct would also have resulted in the deletion of what is now termed Fpr3.

In our paper, we sought mainly to extend our work on the role of the ALX/FPRL2 receptor as an endogenous counterregulator of the innate response by developing an appropriate transgenic mouse model. Such an approach entailed identification of the appropriate murine receptor, but this proved unexpectedly difficult to pin down. Unlike the human formyl-peptide receptor (FPR) family, which has only three members (FPR1, -2, and -3, formerly termed FPR, FPRL1, and FPRL2), of which FPR2 is the accepted receptor for lipoxin A_4 (LXA_4) and Anx-A1 (3), the murine Fpr family comprises at least eight genes (4, 5). Confusingly, two highly (82%) homologous receptors formerly termed Fpr-rs1 and Fpr-rs2 were found also to have strong homology with the human ALX receptor ($\sim$74 and 76%, respectively, at both amino acid and RNA level). Both receptors recognized and responded to the ligand LXA_4 (6, 7), and so either (or perhaps both) Fpr-rs1 and Fpr-rs2 genes could have coded for the receptor(s) we sought.

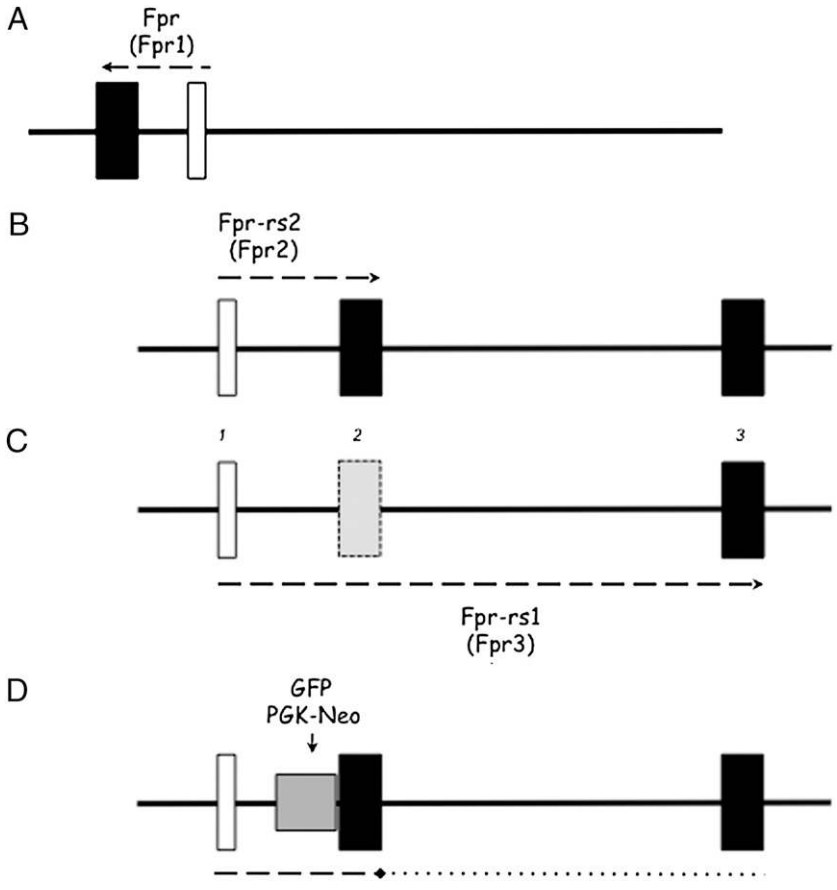

FIGURE 1. Annotation of the mouse genome in the vicinity of the Fpr2 gene. Open boxes, noncoding exons; black boxes, coding exons. Arrangement of the Fpr gene (now called Fpr1) (*A*), which is transcribed from a different strand to Fpr-rs2 (now called Fpr2) (*B*), which is transcribed from exons labeled (for convenience) 1 and 2. *C*, Fpr-rs1 (now called Fpr3) includes exon 1 from Fpr2 and exon 3, skipping exon 2 (shown with dotted line). *D*, In the transgenic strain we generated, the PGK-Neo cassette was inserted in reverse orientation into intron 1 of Fpr2 and the GFP fused in-frame (vector shown in gray) with the ATG start codon. This would have prevented transcriptional read-through of the Fpr3 as well as Fpr2 genes.

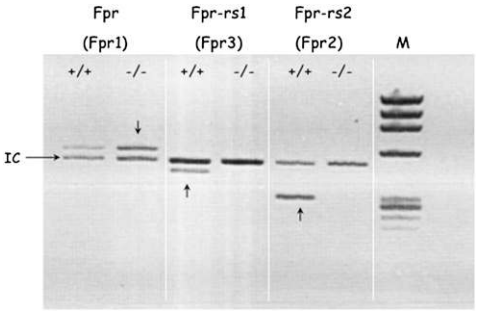

FIGURE 2. Expression of Fpr genes in Fpr2 null mice. Multiplex PCR was used to compare the expression of Fpr1 (formerly Fpr) and Fpr2 (formerly Fpr-rs2) in wild-type and Fpr2 null mice as generated in Ref. 1. Primers were compared with the internal control (IC) gene (18S rRNA). In addition to the deletion of the Fpr2 gene, this strategy also deletes Fpr3, which incorporates exon 2 of Fpr2.

Since its initial description, however, the nomenclature and annotation of the murine Fpr family has changed. Fpr-rs2 was renamed Fpr2, but the situation regarding Fpr-rs1 was more complex. On the basis of the information available at the time of our publication, we originally believed this gene to comprise two isoforms, one of which was subsequently officially designated as Fpr3.

Our current understanding, based upon the latest annotations of the murine gene family, however, is that our targeting strategy would also delete Fpr3 itself because this gene also incorporates an exon found in Fpr2, and so insertion of the GFP reporter and the presence of the pgk-neo cassette in the cds (exon 2) of "Fpr-rs2" (as described in our paper) would prevent expression (Fig. 1) of this gene also. The transcription of the Fpr1 gene is unaffected.

This supposition was confirmed by the multiplex PCR data shown below in Fig. 2, which is an amendment of Fig. 1 from our original publication (1). In Fig. 1 (1), the lane showing the absence from the null animals of (what was then believed by us to be) one of two isoforms of Fpr-rs1 was omitted.

If our current interpretation is correct, the results we reported (1) could be interpreted as being in part due to the deletion of this additional Fpr receptor, and the apparent differences between mouse phenotypes in the two papers may therefore have a logical explanation. Because LXA_4 failed to produce its antimigratory properties in the mouse colony we generated, and the effect of Anx-A1 and its bioactive N-terminal peptide were also substantially diminished or absent (1), it is certainly the case that we functionally deleted the appropriate receptor(s) for our purpose.

Murine Fpr1, Fpr2, and Fpr3 RNA are all expressed in leukocytes, spleen, and lung (4), but there is little (as yet), published on the potential differences in function between the highly homologous Fpr2 and Fpr3 receptors. Interestingly, the selective human FPR3 protein agonist, F2L, loses efficacy in murine cells lacking Fpr2 (8), highlighting the difficulty in attempting a direct correlation between the function of the human and murine gene families.

Ultimately, only further experimental work will clarify biological function of the many Fpr gene products transcribed from this complex locus.

We thank Dr. Charles Mein for his invaluable help and advice on the organization and annotation of the the murine Fpr gene family.

References

1. Dufton, N., R. Hannon, V. Brancaleone, J. Dalli, H. B. Patel, M. Gray, F. D'Acquisto, J. C. Buckingham, M. Perretti, and R. J. Flower. 2010. Anti-inflammatory role of the murine formyl-peptide receptor 2: ligand-specific effects on leukocyte responses and experimental inflammation. *J. Immunol.* 184: 2611–2619.
2. Chen, K., Y. Le, Y. Liu, W. Gong, G. Ying, J. Huang, T. Yoshimura, L. Tessarollo, and J. M. Wang. 2010. A critical role for the g protein-coupled receptor mFPR2 in airway inflammation and immune responses. *J. Immunol.* 184: 3331–3335.
3. Perretti, M., N. Chiang, M. La, I. M. Fierro, S. Marullo, S. J. Getting, E. Solito, and C. N. Serhan. 2002. Endogenous lipid- and peptide-derived anti-inflammatory pathways generated with glucocorticoid and aspirin treatment activate the lipoxin A4 receptor. *Nat. Med.* 8: 1296–1302.
4. Gao, J. L., H. Chen, J. D. Filie, C. A. Kozak, and P. M. Murphy. 1998. Differential expansion of the N-formylpeptide receptor gene cluster in human and mouse. *Genomics* 51: 270–276.
5. Ye, R. D., F. Boulay, J. M. Wang, C. Dahlgren, C. Gerard, M. Parmentier, C. N. Serhan, and P. M. Murphy. 2009. International Union of Basic and Clinical Pharmacology. LXXIII. Nomenclature for the formyl peptide receptor (FPR) family. *Pharmacol. Rev.* 61: 119–161.
6. Takano, T., S. Fiore, J. F. Maddox, H. R. Brady, N. A. Petasis, and C. N. Serhan. 1997. Aspirin-triggered 15-epi-lipoxin A4 (LXA4) and LXA4 stable analogues are potent inhibitors of acute inflammation: evidence for anti-inflammatory receptors. *J. Exp. Med.* 185: 1693–1704.
7. Vaughn, M. W., R. J. Proske, and D. L. Haviland. 2002. Identification, cloning, and functional characterization of a murine lipoxin A4 receptor homologue gene. *J. Immunol.* 169: 3363–3369.
8. Devosse, T., A. Guillabert, N. D'Haene, A. Berton, P. De Nadai, S. Noel, M. Brait, J. D. Franssen, S. Sozzani, I. Salmon, and M. Parmentier. 2009. Formyl peptide receptor-like 2 is expressed and functional in plasmacytoid dendritic cells, tissue-specific macrophage subpopulations, and eosinophils. *J. Immunol.* 182: 4974–4984.

www.jimmunol.org/cgi/doi/10.4049/jimmunol.1090139